Capecitabine efficacy is correlated with TYMP and RB expression in PDX established from triple-negative breast cancers

Elisabetta Marangoni[1], Cécile Laurent[1], Florence Coussy[1,2,3], Rania El-Botty[1], Sophie Château-Joubert[4], Jean-Luc Servely[4,5], Ludmilla de Plater[1], Franck Assayag[1], Ahmed Dahmani[1], Elodie Montaudon[1], Fariba Nemati[1], Justine Fleury[1], Sophie Vacher[3], David Gentien[1], Audrey Rapinat[1], Pierre Foidart[6], Nor Eddine Sounni[6], Agnès Noel[6], Anne Vincent-Salomon[7], Marick Lae[7], Didier Decaudin[1,2], Sergio Roman-Roman[1], Ivan Bièche[3], Martine Piccart[8], Fabien Reyal[1,9,10].

Authors' Affiliations:

[1]Translational Research Department, Institut Curie, PSL Research University, Paris, France; [2] Medical Oncology Department, Institut Curie, PSL Research University, Paris, France; [3]Genetics Department, Institut Curie, PSL Research University, Paris, France; [4] BioPôle Alfort, Ecole Nationale Vétérinaire d'Alfort, Maisons Alfort, France; [5]INRA, PHASE Department, [6]Laboratory of Tumor and Developmental Biology, Groupe Interdisciplinaire de Génoprotéomique Appliqué-Cancer (GIGA-Cancer), University of Liège, Liège 4000, Belgium, [7]Department of Pathology, Institut Curie, PSL Research University, Paris, France, [8]Department of Medical Oncology, Institut Jules Bordet, Université Libre de Bruxelles, Brussels, Belgium, [9]Surgery Department, Institut Curie, PSL Research University; [10]U932, Immunity and Cancer, INSERM, Institut Curie, Paris, France.

Corresponding Author:

Elisabetta Marangoni, Translational Research Department, Institut Curie, 26 rue d'Ulm, Paris 75005, France. E-mail: elisabetta.marangoni@curie.fr Phone: +33 1 56 24 62 42

Running title: RB and TYMP as biomarkers of capecitabine response in TNBC

Keywords: TNBC, residual disease, capecitabine, RB, TYMP

Conflict of interest

The authors declare that they have no competing interests.

Abstract

Purpose: triple-negative breast cancer (TNBC) patients with residual disease after neoadjuvant chemotherapy have a poor outcome. We developed patient-derived xenografts (PDX) from residual tumors to identify efficient chemotherapies and predictive biomarkers in a context of resistance to anthracyclines and taxanes-based treatments.

Experimental Design: PDX were established from residual tumors of primary breast cancer patients treated in neoadjuvant setting. TNBC PDX were treated by anthracyclines, taxanes, platins and capecitabine. Predictive biomarkers were identified by transcriptomic and immunohistological analysis. Downregulation of *RB1* was performed by siRNA in a cell line established from a PDX.

Results: residual TNBC PDX were characterized by a high tumor take, a short latency and a poor prognosis of the corresponding patients. With the exception of BRCA1/2 mutated models, residual PDX were resistant to anthracyclines, taxanes, and platins. Capecitabine, the oral prodrug of 5-FU, was highly efficient in 60% of PDX with two models showing complete responses. Prior treatment of a responder PDX with 5-FU increased expression of thymidylate synthase and decreased efficacy of capecitabine. Transcriptomic and IHC analyses of 32 TNBC PDX, including both residual tumors and treatment-naïve derived tumors, identified RB and TYMP proteins as predictive biomarkers for capecitabine response. Finally, *RB1* knockdown in a cell line established from a capecitabine-responder PDX decreased sensitivity to 5-FU treatment.

Conclusions: we identified capecitabine as efficient chemotherapy in TNBC PDX models established from residual disease and resistant to anthracyclines, taxanes and platins. RB positivity and high expression of TYMP were significantly associated with capecitabine response.

Translational Relevance

Residual disease after neoadjuvant chemotherapy is associated with poor outcome in TNBC patients. There is no standard of care for adjuvant treatment for these patients, and chemotherapy in the metastatic setting is of limited efficacy. We established a panel of PDX from breast residual tumors after neoadjuvant chemotherapy. We identified capecitabine as effective chemotherapy in TNBC PDX with cross-resistance to anthracyclines, taxanes and platins. Prior treatment of PDX by 5-FU resulted in increased thymidylate synthase expression and decreased capecitabine efficacy. Molecular analyses identified RB and TYMP proteins as predictive biomarkers of capecitabine response. In addition, a pharmacodynamic analysis of post-treatment tumors showed strong inhibition of RB-dependent genes in capecitabine responder tumors. These results suggest that RB and TYMP expression in residual breast tumors may help to identify patients more likely to respond to capecitabine in adjuvant or metastatic setting.

Introduction

Triple-negative breast carcinomas (TNBC), which are negative for estrogen/progesterone (ER/PR) receptor expression and lack HER2 overexpression, account for 15% to 20% of breast cancers. TNBC differ from other subtypes of breast cancer in terms of axillary lymph node involvement, locoregional recurrence, time to metastasis (these patients have a high risk of early relapse and much lower survival in the first three to five years after treatment) and patterns of distant recurrence (1). TNBC is emerging as a highly heterogeneous disease in terms of histological features, clinical behavior and sensitivity to systemic treatments (1). It constitutes a major clinical challenge, as there have been no

major improvements in the treatment of this subgroup of tumors, apart from chemotherapy (anthracycline- and taxane-based chemotherapy regimens), which has reduced mortality by about 30% (2).

Cytotoxic chemotherapy is currently the only treatment option for TNBC. For TNBC patients, a pathological complete response (pCR) to NAC is associated with prolonged overall and event-free survival times (3-5). Although the rate of pCR following standard NAC is significantly higher for TNBC as compared to the other breast cancer subtypes, more than 50% of TNBC patients treated in the neoadjuvant setting have residual disease and are associated to an increased risk of distant recurrence, particularly during the first three years after treatment, and a poor outcome. This paradox may be explained by the presence of residual disease in more than half the patients (>60%). At present, there is no standard of care for adjuvant treatment in TNBC patients with residual disease after NAC, and chemotherapy in patients with metastatic disease is of limited efficacy.

Preclinical studies focusing on residual tumors after NAC could provide an important tool to identify efficient therapies and predictive biomarkers in tumors showing resistance to NAC (6). In this study, we established patient-derived xenografts (PDX) from residual breast tumors after NAC and found that capecitabine was an effective chemotherapy agent in 60% of TNBC models. We also identified the expression of thymidylate phosphorylase (TYMP) and RB as biomarkers predictive of the response to capecitabine.

Materials and Methods

Patient-derived xenografts

Female Swiss nude mice were purchased from Charles River (Les Arbresles, France) and maintained under specific pathogen-free conditions. Their care and housing were in accordance with institutional guidelines and the rules of the French Ethics Committee (project authorization no. 02163.02). Patient-derived xenografts were established from primary breast cancer patients with residual

disease after neoadjuvant chemotherapy, with informed consent from the patient, in accordance with published protocols (7, 8). For two patients (#90 and #95) xenografts were established from a local breast cancer recurrence treated by NAC. These two patients were excluded frm the disease-free survival analysis.

Histology and immunohistochemistry status (ER, PR and HER2) was determined for the PDX and compared with that of the patient tumors, as described elsewhere (7, 9). The PDX derived from primary tumors have been described elsewhere (7, 8, 10).

Adriamycin (DOX, doxorubicin, Teva Pharmaceuticals, Paris, France), docetaxel (Sanofi Aventis, Marly-la-Ville, France), cisplatin (CDDP, Teva) and cyclophosphamide (Endoxan, Baxter, Maurepas, France) were administered by the intraperitoneal (ip) route, at doses of 2 mg/kg, 20 mg/kg, 6 mg/kg and 100 mg/kg, respectively, every three weeks. Capecitabine (Xeloda, Roche Laboratories, Nutley, NJ) was administered per os at a dose of 540 mg/kg/day, q5d x 6 weeks. Paclitaxel (Fresenius Kabi France) was administered weekly, at a dose of 20 mg/kg (ip), and bevacizumab (Roche, Boulogne-Billancourt, France) was administered at a dose of 10 mg/kg (ip) every three weeks. Trastuzumab (Roche) was administered weekly, at a dose of 10 mg/kg. Fluorouracil (5-FU) (Fresenius Kabi France) was administered at a dose of 50 mg/kg (ip) and navelbine (Pierre Fabre Laboratories, France) was administered at a dose of 3 mg/kg (iv) every two weeks. The doses for drug combinations were determined in tolerance studies, based on human equivalences (11) and clinical schedules.

Relative tumor volumes (RTVs) and the percent tumor growth inhibition (TGI) were calculated as previously described (7). Kaplan–Meier survival analysis was performed on HBCx-95 xenografts treated with various chemotherapy regimens, with GraphPad Prism software (San Diego, CA). An event was defined as a quadrupling of tumor volume from the initial tumor volume (12).

Percent change in tumor volume was calculated for each tumor as (Vf-V0/V0)*100 where V0 = initial volume (at the beginning of treatment) and Vf= final volume (at the end of treatment). Tumor regression (R) was defined as a decrease in tumor volume of at least 50% taking as reference the

baseline tumor volume; at least a 35% increase in tumor volume identified progressive disease (PD) and responses that were between +35% and -50% were considered as stable disease (SD) (13). Categorical variables were analyzed with Fisher's exact test. The statistical significance of TGI was determined in Mann-Whitney U tests.

Statistical analysis of the patients' clinical data

We analyzed the clinical parameters of 12 patients in the residual disease group (two patients receiving neoadjuvant chemotherapy for local breast cancer relapse were excluded) and 30 patients in the primary tumor group.

The clinical data for the patients are expressed as frequencies for qualitative variables or medians and associated range for quantitative variables. They were compared in Chi-squared or Fisher's exact tests, as appropriate. Disease-free probabilities were estimated by the Kaplan–Meier method, and survival curves were compared in log-rank tests. Analyses were performed with survival and ggplot2 R libraries.

Targeted next-generation sequencing

DNA extraction and targeted next-generation sequencing of TP53, BRCA1 and BRCA2 were performed by the ICGex NGS platform of Institut Curie, as previously described (14). Germline BRCA1 and BRCA2 mutations (BRCA1: p.E849X; BRCA2: p.T1282fs) were present in both the initial tumors and the PDX.

RNA extraction and RT-PCR analysis

RNA extraction and RT-qPCR were performed as previously described (10, 15). For gene normalization, we used the human TATA box-binding protein (TBP, GeBbank accession no. NM_003194). We used protocols for cDNA synthesis and PCR amplification described in detail elsewhere (16, 17). The results are expressed as N-fold differences in target gene expression relative

to the TBP gene. In the pharmacodynamics analysis, these N-fold differences values for each xenograft were subsequently normalized to yield a median value of 1 for the control xenograft group.

Microarray data analysis

GeneChip Human 1.1 ST arrays were hybridized according to Affymetrix recommendations, using the Ambion WT Expression Kit protocol (Life Technologies) and Affymetrix labeling and hybridization kits. All analyses were performed with R software (version 3.3; R Core Team 2017) and Bioconductor packages (version 3.4) (18). Arrays were normalized according to the RMA normalization procedure from oligo package (19). Differential expression between PDX responding and resistant to capecitabine was assessed by a linear model method, with the Limma package (20). We used the false discovery rate (FDR) procedure to adjust for multiple testing. We considered log fold changes in expression > 1.5, and p-values < 0.05 to be statistically significant.

RB1 silencing and cell proliferation assays

The HBCc-12A cell line was established from the residual TNBC PDX HBCx-12A by mechanical dissociation and removal of cellular debris and erythrocytes. The HBCc-12A cell line and the HBCx-12A PDX were genotyped with the GenePrint® 10 System (#B9510, Promega) that allows coamplification and three-color detection of nine human loci. The cell line was grown at 37°C in DMEM Glutamax medium supplemented with 10% Fetal Bovine Serum, 1% Penicillin Streptomycine, 1% Hepes Buffer, 1% Sodium Pyruvate and 10 µg/ml Insulin (Sigma) .

HBCc-12A cells were transfected with 20 nM siRNA against RB1 (SI00007091, QIAGEN) and AllStars siRNA as negative control (SI03650318, QIAGEN) using INTERFERin reagent (POL409-50, Ozyme) in Opti-MEM medium (Life Technologies), according to the manufacturers' instructions.

Cells were plated in duplicate into 96-well culture plates at a density of $7x10^3$ cells per well and left overnight. siRNA and 5-FU were added 24H and 30H after seeding and on day 5 cell proliferation was

determined by MTT assay (3-(4,5-dimethylthiazol-2-yl)-2,5-diphenyltetrazolium bromide) (MTT; M-2128, Sigma).

Western blot

For western blot analyses, 115x 10^3 HBCc-12A cells were plated into 6-well culture plates. siRNA and 5-FU were added at the same concentrations and timelines of MTT proliferation assays. Proteins were extracted as described previously (8). Lysates were resolved on 4–12% TGX gels (Bio-Rad®), transferred into nitrocellulose membranes (Bio-Rad®) and immunoblotted with rabbit antibodies against GAPDH (#2118, Cell Signaling Technology, Leiden, The Netherlands), Rb (#9309, Cell Signaling Technology), P-Rb (#9308, Cell Signaling Technology). After washes, membranes were incubated with the appropriate secondary antibodies horseradish peroxidase-conjugated affinity-purified goat anti–rabbit (111-035-045, Jackson ImmunoResearch Laboratories, Inc., Interchim).

IHC

Xenografted tumors were fixed in 10% neutral buffered formalin, embedded in paraffin and stained with hematoxylin and eosin. Immunostaining was performed on a Discovery XT Platform (Ventana Medical System, Tucson, Arizona, USA, part of Roche Diagnostics) (17). The slides were incubated with a polyclonal rabbit antibody against TYMP (#HPA001072, Sigma, St. Quentin, France), a monoclonal mouse antibody against RB (#9309, clone 4H1, Cell Signaling Technology, Leiden, The Netherlands) and a monoclonal rabbit antibody against TYMS (#9045, Ozyme, Saint-Quantin Yvelines, France). Slides immunostained with mouse and rabbit IgG were used as negative controls. Slides were incubated with anti-rabbit/mouse secondary antibodies (horseradish peroxidase complex) and DAB (3,3'-diaminobenzidine tetrahydrochloride) as the substrate for color development (ChromoMap Kit with Anti rabbit OmniMap, Ventana Medical System). TYMP immunostaining was assessed by determining the intensity and distribution of stained cancer cells, as previously described

(21). Immunostaining intensity was scored as follows: 0, negative staining; 1, weak staining; 2, moderate staining; and 3, strong staining. Immunostaining intensity scores were grouped into three classes, as follows: 1) ≤33% of the tumor cells stained; 2), 33-66% of the tumor cells stained; and 3) 66-100% of the tumor cells stained. Summed scores were also obtained by adding the scores for two parameters (21).

Results

Residual tumors are characterized by high take rates and poor survival of the corresponding patients

We established 22 PDX by transplanting 53 breast tumors from patients with residual disease after NAC. The take rates for the ER+, HER2+ and triple-negative subtypes were 23%, 22% and 78%, respectively (Supplementary Table 1). When compared to PDX derived from treatment-naïve primary tumors, previously reported (7, 9), take rates of residual tumors were higher for ER+ and triple-negative subtypes (Fig. 1A and Supplementary Table S1). In the TNBC group, median PDX latency after engraftment was 67 days for residual tumors, versus 160 days for treatment-naïve primary tumors (Fig. 1B). With a high tumor take and a short latency, residual TNBC PDX may provide an opportunity for preclinical testing of anticancer agents prior to relapse in patients. We therefore retrospectively compared the metastasis-free survival (MFS) of the patients with the latency periods of the 14 PDX established from the residual tumours (Fig. 1C). Ten of these patients presented a recurrence of metastatic disease, three remain metastasis-free and one died five months after mastectomy (HBC-12A, an 89-year-old patient). PDX latencies were considerably shorter than MFS for eight patients ($p=0.021$, paired t-test).

The clinical characteristics of patients in the residual disease and primary tumors groups are summarized in Supplementary Table 2 and Supplementary Figure 1. Prognosis was worse in the

residual disease group of patients, for whom survival was 28% at 25 months, versus 75% for the patients in the primary tumor group (p=0.048, log-rank test) (Fig. 1D).

These results highlight the aggressive phenotype of residual tumors, with high tumor take rates, a short tumor latency during PDX establishment and low survival of the corresponding patients.

Residual tumor PDX are resistant to anthracyclines, docetaxel and cisplatin, but respond to capecitabine

We determined the response to chemotherapy in 10 PDX derived from residual tumors, and compared this response with that of PDX derived from primary tumors (7). The chemotherapy regimens used were AC (adriamycin plus cyclophosphamide), docetaxel, cisplatin and capecitabine. Only 10%, 20% and 0% of residual TNBC PDX responded to AC, cisplatin, and docetaxel, with a TGI of at least 90%, whereas 50%, 52% and 10% of treatment-naïve TNBC PDX responded to these treatments (Fig.1E). Conversely, residual TNBC PDX displayed a higher frequency of response to capecitabine (60%) as compared to treatment-naïve PDX (36%).

Table 1 summarizes the NAC administered to patients, tumor histology, status for BRCA1/2 and TP53 mutations and response to chemotherapy, as assessed by tumor growth inhibition (TGI) and adapted RECIST criteria (13), for 10 residual TNBC PDX.

Only one residual PDX responded to AC with a TGI≥ 90%, none responded to docetaxel and two (one with a BRCA1 mutation and the other with a BRCA2 mutation) responded to cisplatin (with tumor regression observed in only one of these cases)(Table 1 and Supp. Fig. S2A).

Six of the 10 residual PDX responded to capecitabine with a TGI≥90: four (HBCx-12A, HBCx-63, HBCx-92 and HBCx106) with stable disease and 2 models with tumor regression (HBCx-39 and HBCx-95) (Table 1). Three of the four capecitabine-resistant PDX corresponded to metaplastic breast cancer. The drug response profiles of 3 capecitabine-responder PDX are illustrated in Figure 1F. Response to capecitabine was homogeneous in the different mice (Fig. 1G). HBCx-95 capecitabine-treated xenografts showed complete responses at day 40: the xenografts of this model were monitored for

10 months after the end of treatment. A Kaplan-Meier survival curve (Supp. Fig. S2B) showed that event-free survival was greater for animals treated with capecitabine than for animals receiving other types of chemotherapy (p=0.0004, log-rank test).

The efficacy of capecitabine in PDX is decreased by prior treatment

In the advanced setting, capecitabine is usually administered as a second or third line treatment. We hypothesized that prior treatment of tumors with a different chemotherapy regimen might affect the response to capecitabine. We tested this hypothesis in one residual TNBC PDX, through the sequential administration of chemotherapies administered to the patient in the adjuvant and metastatic settings. Patient #63 received FEC and docetaxel as NAC, followed by 5-FU and navelbine as an adjuvant treatment, then paclitaxel + bevacizumab (first line) and capecitabine (second line) in the metastatic setting (Fig. 2A). We administered the same treatments sequentially to the HBCx-63 PDX, established from the residual tumor, and compared it to the efficacy of capecitabine in non-pretreated tumor. Results are shown in Figure 2B: capecitabine given in xenografts pre-treated by 5-FU + navelbine or by paclitaxel + bevacizumab resulted in progressive disease in 4/5 and 6/6 xenografts (mean of 144% and 130%, respectively). By contrast, 7/9 xenografts treated with capecitabine without prior treatment displayed stable disease, one progressive disease and one tumor regression (mean=14%). Thus, prior treatment by 5-FU and navelbine decreased capecitabine efficacy.

We next analyzed the expression of two enzymes whose expression may influence capecitabine response: thymidylate synthase (TYMS), the target enzyme for 5-FU, and thymidylate phosphorylase (TYMP), an enzyme involved in the metabolism of 5-FU and capecitabine (22). TYMS expression was increased after treatment by 5-FU and navelbine and this increase was maintained in xenografts treated by paclitaxel and bevaciuzumab (Fig. 2C). By contrast, TYMP expression was unchanged by the different treatments (data not shown).

Anti-tumor activity of capecitabine is significantly correlated with expression of RB and thymidylate phosphorylase proteins in a large panel of breast cancer PDX

For the identification of markers predictive of capecitabine response, we combined the capecitabine response data for 10 residual TNBC PDX with those obtained from 22 primary tumor-derived TNBC PDX previously determined (unpublished data). The responses to capecitabine treatment of the 32 TNBC PDX are represented as waterfall plots in Figure 3A: in 15 PDX, capecitabine treatment resulted in stable disease or tumor regression, whereas in the other 17 PDX, it resulted in progressive disease. To identify genes associated with the capecitabine response, we performed a differential analysis of gene expression microarray datasets available for 25 TNBC PDX (15 resistant and 10 sensitive). Hierarchical clustering based on 37 genes (17 upregulated and 20 downregulated in sensitive PDX) grouped 100% of sensitive PDX together (Fig. 3B). The 37 genes concerned are listed in Supplementary Table S3. Three of these genes encode proteins involved in cell-cycle regulation: *RB1* and *CCND1*, which were upregulated in responder models, and *CDKN2A*, which was upregulated in resistant models. Among genes implicated in capecitabine metabolism *(TYMP, TYMS, TK1, DPYD),* only *TYMP* expression was higher in responder models, although the fold change did not pass the threshold for global differential analysis (Supp. Fig. S3).

To validate RB at the protein level, we analyzed its expression by IHC in the 32 TNBC PDX. RB protein was detected in all 15 (100%) responder PDX and in 6/17 resistant (35%) PDX (Fig. 3C and 3D). Positive and negative predictive values were 71% and 100%, respectively (p=0.0001, Fisher's exact test).

We then quantified TYMP protein expression in the 32 TNBC PDX by determining the IHC H-score (21). Examples of negative and positive TYMP IHC results are shown in Figure 3E. Thymidine phosphorylase IHC H-score was significantly higher in responder tumors (Fig. 3F). Median TYMP IHC H-score was 4.25 (range: 0–6): 80% of the responding PDX had TYMP expression scores ≥4.25 and 76% of resistant PDX had scores < 4.25. Positive and negative predictive values were 75% and 81%, respectively (*p*=0.0038; Fisher's exact test). Among the 6 RB positive PDX that did not respond to

capecitabine, 5 showed no or low expression of TYMP (data not shown). The combination of RB positivity and a TYMP score> 4.25 had a positive predictive value of 92% and a negative predictive value of 100%, accurately predicting response in 12/15 xenografts and resistance in 8/17.

Finally, we assessed capecitabine efficacy in one PDX derived from a patient with HER2-positive breast cancer treated with trastuzumab in the pre-operative setting (HBCx-73). The xenograft was Rb-positive and expressed high levels of TYMP (Supp. Fig. S4A). Capecitabine had strong antitumor activity against this xenograft (TGI=99%), whereas trastuzumab did not arrest tumor growth (Supp. Fig. S4B).

Tumor growth inhibition is correlated with a strong decrease in the expression of various RB-dependent genes in capecitabine-treated xenografts

RB plays a critical role in coordinating the expression of genes required for cell-cycle progression through interaction with the transcription factor E2F. We therefore looked at the correlation between capecitabine's efficacy and the expression changes of 8 genes included in the "RB gene expression signature" and involved in cell proliferation (*CCNA2, CCNB1, TOP2A, TTK, PLK1* and *AURKA*) and nucleotides metabolism *(TYMS, TK1*) (23). We analyzed control and post-treatment xenografts of 7 PDX, including both capecitabine-resistant and capecitabine-sensitive PDX (Fig. 4A). The expression levels of the eight genes, determined by RT-PCR, are shown in Supplementary Figure S5. A heat-map representing the fold-change difference between capecitabine-treated and control xenografts is shown in Figure 4B. All genes were strongly downregulated in the three RB-positive PDX with the highest levels of tumor growth inhibition (HBCx-63, HBCx-12A and HBCx-39), whereas no change was found in the three PDX in which capecitabine had little or no effect. The correlation between fold-change differences in gene expression and tumor growth inhibition by capecitabine is shown in Figure 4C and was statistically significant for all genes.

Inhibition of RB1 gene decreases response to 5-FU in vitro

We tested whether RB1 inhibition could have an impact on capecitabine reponse in the HBCc-12A cell line, established from the RB positive HBCx-12A PDX (residual tumor derived PDX). This PDX responds to capecitabine with a TGI of 96% (stable disease with recist criteria) (Fig. 5A). We performed a cell viability assay to determine the *in vitro* response of the cell line to 5-FU: the cell line showed a IC50 of 33 μM (Fig. 5B). The cell line was then transfected with 2 different siRNA directed against RB1 or control (scramble siRNA) and exposed to 40 μM of 5-FU for 120H. Western blot analysis demonstrated downregulation of RB protein in cell exposed to siRB1 and siRB2, with an increased inhibition for siRB1, in both untreated and 5-FU treated cells (Fig. 5C). Phosphorylation of RB protein was inhibited by 5-FU. Inhibition of RB1 decreased sensitivity to 5-FU of 40% as assessed by the MTT viability assay (the increased viability was greater for siRB1 as compared to siRB2) (Fig. 5D). In summary, these results show that RB has a role in determining the cellular response to 5-FU treatment.

Discussion

We established a cohort of breast cancer PDX models by engrafting residual tumors after NAC. Residual TNBC PDX had a higher tumor take rate and a shorter latency than TNBC PDX derived from treatment-naïve breast cancers. Both these characteristics are suggestive of an aggressive phenotype. These results are similar to those reported by McAuliffe *et al* who showed that take rates were higher for breast cancers treated in the neoadjuvant setting (24). The aggressiveness of these tumors was confirmed by the poor outcomes of the corresponding patients. In more than half the TNBC patients, PDX latency was shorter than metastasis-free survival. The residual tumor PDX therefore becomes available for *in vivo* drug testing over a time frame compatible with clinical decision-making concerning first-line chemotherapy. Furthermore, residual TNBC PDX were resistant to anthracyclines and docetaxel-based chemotherapy. As these drugs were given to patients in the

neoadjuvant setting, in which they were of limited efficacy, the resistance phenotype of the patients' tumors is maintained and reproduced in xenograft models. Residual tumor PDX were also resistant to cisplatin, with the exception of PDX established from BRCA1/2-mutated breast cancers. Despite the small size of this series of xenograft models, this finding indicates that residual tumors display a multidrug resistance phenotype extending to different chemotherapy classes, including anthracyclines, cyclophosphamide, docetaxel and cisplatin. It also suggests that patients with BRCA1- and BRCA2-mutated tumors may still respond to platin-based chemotherapies. The patient with the BRCA1-mutated tumor has not yet relapsed, and the patient carrying the BRCA2-mutated tumor displayed a partial response to six cycles of first-line treatment with paclitaxel and carboplatin. However, given the small number of cases, these results require confirmation in a larger cohort.

Responses to capecitabine were observed in six of the 10 residual tumor-derived PDXs displaying cross-resistance to anthracyclines, docetaxel and cisplatin. Three of the four capecitabine-resistant PDX were established from metaplastic breast cancers, a histological subtype of TNBC known to be particularly aggressive and resistant to chemotherapy (25).

These findings are of particular interest for several reasons. Firstly, they are consistent with the results of a recent clinical trial (CREATE-X) demonstrating the efficacy of adjuvant capecitabine treatment in TNBC patients with residual invasive disease after neoadjuvant chemotherapy (26). Secondly, capecitabine treatment is well tolerated and may be compatible with adjuvant treatment in patients with a high risk of tumor recurrence. The FinXX trial also reported beneficial effects on survival in TNBC patients treated with a capecitabine-containing regimen in the adjuvant setting (27). In the CREATE-X trial, TNBC disease-free survival was 69.8% in the capecitabine group, versus 56.1% in the control group (26). Thus, a large proportion of patients remained that did not benefit from adjuvant capecitabine treatment. Predictive biomarkers are crucial for identifying the patients most likely to benefit from treatment.

Based on the analysis of transcriptomic data, we identified and validated RB as a biomarker predictive of the response to capecitabine in TNBC PDX. RB is a tumor suppressor protein that

regulates cell-cycle progression by preventing entry into the mitotic phase (28). It may be inactivated by hyperphosphorylation or protein loss, both of which disrupt its association with the transcription factor E2F, facilitating the expression of a transcriptional program leading to progression through S-phase and mitosis (29). RB is also a key regulator of cell-cycle arrest upon DNA damage (30). The finding that capecitabine efficacy is correlated with RB expression may be explained by the role of this protein in cell-cycle control and the checkpoint response to chemotherapy. Consistent with this hypothesis, RB reconstitution in RB-deficient lung cancer cell lines re-establishes the regulation of REB/E2F target genes and restores the G1 checkpoint response to chemotherapy regimens including 5-FU (31). Similarly, inactivation of *RB1* gene by siRNA in a cell line derived from a capecitabine-responder PDX decreased sensitivity to 5-FU, further supporting a role of RB in determining the response to 5-FU/capecitabine.

In addition to its role in canonical cell cycle-dependent regulation, RB also inhibits cell proliferation by regulating nucleotide metabolism by inhibiting enzymes involved in dNTP synthesis. The absence of functional RB leads to a deregulation of the expression of dNTP enzymes (such as TYMS) and antimetabolite resistance (32). Li *et al.* demonstrated that a lack of functional RB increases resistance to antimetabolite drugs in human sarcoma cells, by increasing the expression of the *DHFR* and *TYMS* genes, both of which are under the control of the E2F factor and targeted by antimetabolite chemotherapy (33). The expression of genes encoding proteins involved in nucleotide metabolism (TYMS) and the RB-dependent S-phase DNA damage response (CCNA2) (34) was strongly inhibited in RB-positive models treated with capecitabine, suggesting that the canonical and metabolic regulation of cell proliferation may together account for the observed antitumor effects of capecitabine.

From the analysis of transcriptomic data, RB1 and CDKN2A expression appeared inversely correlated, a finding that is in line with previous reports (35). CDKN2A gene encodes the p16(INK4a) protein that plays an important role in cell cycle through the regulation of the cyclin-dependent kinase (CDK) 4/6 and cyclin D complexes. Loss of p16(INK4a) can occur by genetic or epigenetic mechanisms and results in Rb protein activation, leading to unchecked cellular proliferation (36). Evaluation of

p16(INK4a) expression by immunohistochemistry analyses in TNBC PDX will be necessary in order to validate it as potential biomarker of capecitabine resistance.

Finally, an association has been found between the RB pathway and chemotherapy response in breast cancer patients (28). In metastatic breast cancer, mutations of the RB gene are associated with a poor response to anthracyclines (37, 38). RB pathway inactivation is predictive of resistance to DNA damage-based treatments in locally advanced breast cancer (39).

Capecitabine is converted to 5-FU in cancer cells TYMP enzyme (40). Thymidine phosphorylase also activates 5-FU, by converting it to 5-fluoro-2'-deoxyuridine, a precursor of FdUMP that inhibits the TYMS enzyme, responsible for *de novo* thymidylate synthesis (22). Accordingly, capecitabine-based chemotherapies have been reported to be more effective in tumors with high levels of TYMP (41-44). Expression of TYMP, as assessed by IHC, was significantly correlated with the response to capecitabine in the cohort of 32 TNBC PDX (including PDX derived from both residual and treatment-naïve tumors). These results are consistent with those of various different clinical studies showing a correlation between TYMP expression and response to capecitabine in metastatic breast cancer patients previously treated with anthracyclines and taxanes (42, 45).

The evaluation of TYMP and RB as predictive biomarkers could be translated into clinical practice. Immunohistochemical analyses of one of these two biomarkers on residual tumors at surgery could identify those patients likely to benefit from adjuvant capecitabine treatment. Retrospective validations of these biomarkers in clinical trials evaluating capecitabine against controls (like the CREATE-X study) could also be used to provide support for our results.

Our results may also have implications for the advanced cancer setting, as capecitabine is usually given as a second- or third-line treatment in patients with recurrences after NAC (46, 47). The efficacy of capecitabine was decreased after pre-treatment of tumors with 5-FU and this was associated to increased expression of TYMS. The up-regulation of TYMS in 5-FU treated tumors is consistent with previous finding in cell lines and tumors and can be explained by the inhibition of a negative feedback mechanism in which TYMS protein inhibits the translation of TYMS mRNA (48).

When bound to the active metabolite of 5-FU (FdUMP), TYMS is not able to bind to its mRNA which results in increased protein expression (49). This constitutes a mechanism of acquired resistance to 5-FU (50, 51). This case suggests that capecitabine might be more effective if introduced earlier, as adjuvant or first line treatment, and raises the question of giving 5-FU prior to capecitabine.

In conclusion, we have developed a panel of PDX models from breast cancer patients with residual disease after neoadjuvant treatment. These chemoresistant PDX provided us with an opportunity to identify effective treatment strategies that might improve the survival of patients with a high risk of relapse and poor prognosis. We showed that capecitabine was effective against 60% of TNBC PDXs derived from tumors previously treated with anthracyclines and taxanes, and we identified TYMP and RB expression as putative biomarkers predictive of the response to capecitabine.

Acknowledgments

This work was supported by grants from the Association pour la Recherche Contre le Cancer (ARC) and the Parisian Alliance of Cancer Research Institutes (PACRI). High-throughput sequencing was performed at the ICGex NGS platform of the Institut Curie, which is supported by the ANR-10-EQPX-03 (Equipx) and ANR-10-INBS-09-08 (France Génomique Consortium) grants from the Agence Nationale de la Recherche (“Investissements d’Avenir" program), Canceropole Ile-de-France and the SiRIC-Curie program - SiRIC Grant “INCa-DGOS- 4654”. We thank the animal platform of the Institut Curie (Isabelle Grandjean) and Julie Sappa of Alex Edelman & Associates for her help in correcting the English version of the manuscript.

References

1. Bianchini G, Balko JM, Mayer IA, Sanders ME, Gianni L. Triple-negative breast cancer: challenges and opportunities of a heterogeneous disease. Nat Rev Clin Oncol. 2016;13:674-90.
2. Dent R, Trudeau M, Pritchard KI, Hanna WM, Kahn HK, Sawka CA, et al. Triple-negative breast cancer: clinical features and patterns of recurrence. Clin Cancer Res. 2007;13:4429-34.
3. Carey LA, Dees EC, Sawyer L, Gatti L, Moore DT, Collichio F, et al. The triple negative paradox: primary tumor chemosensitivity of breast cancer subtypes. Clin Cancer Res. 2007;13:2329-34.
4. Liedtke C, Mazouni C, Hess KR, Andre F, Tordai A, Mejia JA, et al. Response to neoadjuvant therapy and long-term survival in patients with triple-negative breast cancer. J Clin Oncol. 2008;26:1275-81.
5. Cortazar P, Zhang L, Untch M, Mehta K, Costantino JP, Wolmark N, et al. Pathological complete response and long-term clinical benefit in breast cancer: the CTNeoBC pooled analysis. The Lancet. 2014;384:164-72.
6. Ademuyiwa FO, Ellis MJ, Ma CX. Neoadjuvant therapy in operable breast cancer: application to triple negative breast cancer. J Oncol. 2013;2013:219869.
7. Marangoni E, Vincent-Salomon A, Auger N, Degeorges A, Assayag F, de Cremoux P, et al. A new model of patient tumor-derived breast cancer xenografts for preclinical assays. Clin Cancer Res. 2007;13:3989-98.
8. Hatem R, El Botty R, Chateau-Joubert S, Servely JL, Labiod D, de Plater L, et al. Targeting mTOR pathway inhibits tumor growth in different molecular subtypes of triple-negative breast cancers. Oncotarget. 2016;7:48206-19.
9. Cottu P, Marangoni E, Assayag F, de Cremoux P, Vincent-Salomon A, Guyader C, et al. Modeling of response to endocrine therapy in a panel of human luminal breast cancer xenografts. Breast Cancer Res Treat. 2012;133:595-606.
10. Reyal F, Guyader C, Decraene C, Lucchesi C, Auger N, Assayag F, et al. Molecular profiling of patient-derived breast cancer xenografts. Breast Cancer Res. 2012;14:R11.
11. Reagan-Shaw S, Nihal M, Ahmad N. Dose translation from animal to human studies revisited. FASEB J. 2008;22:659-61.
12. Houghton PJ, Morton CL, Tucker C, Payne D, Favours E, Cole C, et al. The pediatric preclinical testing program: description of models and early testing results. Pediatr Blood Cancer. 2007;49:928-40.

13. Bertotti A, Migliardi G, Galimi F, Sassi F, Torti D, Isella C, et al. A molecularly annotated platform of patient-derived xenografts ("xenopatients") identifies HER2 as an effective therapeutic target in cetuximab-resistant colorectal cancer. Cancer Discov. 2011;1:508-23.
14. Euceda LR, Hill DK, Stokke E, Hatem R, El Botty R, Bieche I, et al. Metabolic Response to Everolimus in Patient-Derived Triple-Negative Breast Cancer Xenografts. J Proteome Res. 2017;16:1868-79.
15. Bieche I, Parfait B, Le Doussal V, Olivi M, Rio MC, Lidereau R, et al. Identification of CGA as a novel estrogen receptor-responsive gene in breast cancer: an outstanding candidate marker to predict the response to endocrine therapy. Cancer Res. 2001;61:1652-8.
16. Tozlu S, Girault I, Vacher S, Vendrell J, Andrieu C, Spyratos F, et al. Identification of novel genes that co-cluster with estrogen receptor alpha in breast tumor biopsy specimens, using a large-scale real-time reverse transcription-PCR approach. Endocr Relat Cancer. 2006;13:1109-20.
17. Hatem R, Labiod D, Chateau-Joubert S, de Plater L, El Botty R, Vacher S, et al. Vandetanib as a potential new treatment for estrogen receptor-negative breast cancers. Int J Cancer. 2016;138:2510-21.
18. Huber W, Carey VJ, Gentleman R, Anders S, Carlson M, Carvalho BS, et al. Orchestrating high-throughput genomic analysis with Bioconductor. Nat Methods. 2015;12:115-21.
19. Carvalho BS, Irizarry RA. A framework for oligonucleotide microarray preprocessing. Bioinformatics. 2010;26:2363-7.
20. Smyth GK, Michaud J, Scott HS. Use of within-array replicate spots for assessing differential expression in microarray experiments. Bioinformatics. 2005;21:2067-75.
21. Kim KW, Kwon HC, Kim SH, Oh SY, Lee S, Lee JH, et al. Prognostic significance of thymidylate synthase, thymidine phosphorylase and dihydropyrimidine dehydrogenase expression in biliary tract cancer patients receiving adjuvant 5-fluorouracil-based chemotherapy. Mol Clin Oncol. 2013;1:987-94.
22. Longley DB, Harkin DP, Johnston PG. 5-fluorouracil: mechanisms of action and clinical strategies. Nat Rev Cancer. 2003;3:330-8.
23. Ertel A, Dean JL, Rui H, Liu C, Witkiewicz AK, Knudsen KE, et al. RB-pathway disruption in breast cancer: differential association with disease subtypes, disease-specific prognosis and therapeutic response. Cell Cycle. 2010;9:4153-63.
24. McAuliffe PF, Evans KW, Akcakanat A, Chen K, Zheng X, Zhao H, et al. Ability to Generate Patient-Derived Breast Cancer Xenografts Is Enhanced in Chemoresistant Disease and Predicts Poor Patient Outcomes. PLoS One. 2015;10:e0136851.
25. Shah DR, Tseng WH, Martinez SR. Treatment options for metaplastic breast cancer. ISRN Oncol. 2012;2012:706162.
26. Masuda N, Lee SJ, Ohtani S, Im YH, Lee ES, Yokota I, et al. Adjuvant Capecitabine for Breast Cancer after Preoperative Chemotherapy. N Engl J Med. 2017;376:2147-59.
27. Joensuu H, Kellokumpu-Lehtinen PL, Huovinen R, Jukkola-Vuorinen A, Tanner M, Kokko R, et al. Adjuvant Capecitabine in Combination With Docetaxel, Epirubicin, and Cyclophosphamide for Early Breast Cancer: The Randomized Clinical FinXX Trial. JAMA Oncol. 2017.
28. Knudsen ES, Knudsen KE. Tailoring to RB: tumour suppressor status and therapeutic response. Nat Rev Cancer. 2008;8:714-24.
29. Witkiewicz AK, Knudsen ES. Retinoblastoma tumor suppressor pathway in breast cancer: prognosis, precision medicine, and therapeutic interventions. Breast Cancer Res. 2014;16:207.
30. Harrington EA, Bruce JL, Harlow E, Dyson N. pRB plays an essential role in cell cycle arrest induced by DNA damage. Proc Natl Acad Sci U S A. 1998;95:11945-50.
31. Reed MF, Zagorski WA, Knudsen ES. RB activity alters checkpoint response and chemosensitivity in lung cancer lines. J Surg Res. 2007;142:364-72.
32. Angus SP, Wheeler LJ, Ranmal SA, Zhang X, Markey MP, Mathews CK, et al. Retinoblastoma tumor suppressor targets dNTP metabolism to regulate DNA replication. J Biol Chem. 2002;277:44376-84.

33. Li W, Fan J, Hochhauser D, Banerjee D, Zielinski Z, Almasan A, et al. Lack of functional retinoblastoma protein mediates increased resistance to antimetabolites in human sarcoma cell lines. Proc Natl Acad Sci U S A. 1995;92:10436-40.
34. Knudsen KE, Booth D, Naderi S, Sever-Chroneos Z, Fribourg AF, Hunton IC, et al. RB-dependent S-phase response to DNA damage. Mol Cell Biol. 2000;20:7751-63.
35. Aagaard L, Lukas J, Bartkova J, Kjerulff AA, Strauss M, Bartek J. Aberrations of p16Ink4 and retinoblastoma tumour-suppressor genes occur in distinct sub-sets of human cancer cell lines. Int J Cancer. 1995;61:115-20.
36. Witkiewicz AK, Knudsen KE, Dicker AP, Knudsen ES. The meaning of p16(ink4a) expression in tumors: functional significance, clinical associations and future developments. Cell Cycle. 2011;10:2497-503.
37. Berge EO, Knappskog S, Lillehaug JR, Lonning PE. Alterations of the retinoblastoma gene in metastatic breast cancer. Clin Exp Metastasis. 2011;28:319-26.
38. Berge EO, Knappskog S, Geisler S, Staalesen V, Pacal M, Borresen-Dale AL, et al. Identification and characterization of retinoblastoma gene mutations disturbing apoptosis in human breast cancers. Mol Cancer. 2010;9:173.
39. Knappskog S, Berge EO, Chrisanthar R, Geisler S, Staalesen V, Leirvaag B, et al. Concomitant inactivation of the p53- and pRB- functional pathways predicts resistance to DNA damaging drugs in breast cancer in vivo. Mol Oncol. 2015;9:1553-64.
40. Miwa M, Ura M, Nishida M, Sawada N, Ishikawa T, Mori K, et al. Design of a novel oral fluoropyrimidine carbamate, capecitabine, which generates 5-fluorouracil selectively in tumours by enzymes concentrated in human liver and cancer tissue. Eur J Cancer. 1998;34:1274-81.
41. Schuller J, Cassidy J, Dumont E, Roos B, Durston S, Banken L, et al. Preferential activation of capecitabine in tumor following oral administration to colorectal cancer patients. Cancer Chemother Pharmacol. 2000;45:291-7.
42. Lee SJ, Choi YL, Park YH, Kim ST, Cho EY, Ahn JS, et al. Thymidylate synthase and thymidine phosphorylase as predictive markers of capecitabine monotherapy in patients with anthracycline- and taxane-pretreated metastatic breast cancer. Cancer Chemother Pharmacol. 2011;68:743-51.
43. Koizumi W, Okayasu I, Hyodo I, Sakamoto J, Kojima H, Clinical Study Group of C. Prediction of the effect of capecitabine in gastric cancer by immunohistochemical staining of thymidine phosphorylase and dihydropyrimidine dehydrogenase. Anticancer Drugs. 2008;19:819-24.
44. Kobashi N, Matsumoto H, Zhao S, Meike S, Okumura Y, Abe T, et al. The Thymidine Phosphorylase Imaging Agent 123I-IIMU Predicts the Efficacy of Capecitabine. J Nucl Med. 2016;57:1276-81.
45. Andreetta C, Puppin C, Minisini A, Valent F, Pegolo E, Damante G, et al. Thymidine phosphorylase expression and benefit from capecitabine in patients with advanced breast cancer. Ann Oncol. 2009;20:265-71.
46. Gavilá J, Lopez-Tarruella S, Saura C, Muñoz M, Oliveira M, De la Cruz-Merino L, et al. SEOM clinical guidelines in metastatic breast cancer 2015. Clinical and Translational Oncology. 2015;17:946-55.
47. Cardoso F, Costa A, Senkus E, Aapro M, André F, Barrios CH, et al. 3rd ESO–ESMO International Consensus Guidelines for Advanced Breast Cancer (ABC 3). Annals of Oncology. 2016:mdw544.
48. Chu E, Koeller DM, Johnston PG, Zinn S, Allegra CJ. Regulation of thymidylate synthase in human colon cancer cells treated with 5-fluorouracil and interferon-gamma. Mol Pharmacol. 1993;43:527-33.
49. Chu E, Koeller DM, Casey JL, Drake JC, Chabner BA, Elwood PC, et al. Autoregulation of human thymidylate synthase messenger RNA translation by thymidylate synthase. Proc Natl Acad Sci U S A. 1991;88:8977-81.
50. Ahn JY, Lee JS, Min HY, Lee HY. Acquired resistance to 5-fluorouracil via HSP90/Src-mediated increase in thymidylate synthase expression in colon cancer. Oncotarget. 2015;6:32622-33.

51. Peters GJ, Backus HH, Freemantle S, van Triest B, Codacci-Pisanelli G, van der Wilt CL, et al. Induction of thymidylate synthase as a 5-fluorouracil resistance mechanism. Biochim Biophys Acta. 2002;1587:194-205.

Tables Legend

Table 1: Histology, mutation and response to chemotherapy in TNBC PDX derived from residual tumors after neoadjuvant chemotherapy

PDX	Neoadjuvant treatment of TNBC patients	Tumor Histology	TP53 and BRCA1/2 mutations	PDX response: % TGI and RECIST criteria			
				AC	docetaxel	cisplatin	capecitabine
HBCx-12A	docetaxel	IDC	None	44 (PD)	28 (PD)	0 (PD)	**96 (SD)**
HBCx-39	EC + docetaxel	IDC	TP53	36 (PD)	0 (PD	16 (PD)	**98 (R)**
HBCx-48	FEC docetaxel	IDC	TP53	30 (PD)	0 (PD)	40 (PD)	37 (PD)
HBCx-63	FEC docetaxel	IDC	TP53	74 (PD)	30 (PD)	86 (PD)	**96 (SD)**
HBCx-66	FEC docetaxel	MBC	BRCA1	**94 (R)**	0 (PD)	**98 (R)**	41.4 (PD)
HBCx-69	FEC docetaxel	MBC	TP53	31 (PD)	50 (PD)	64 (PD)	55 (PD)
HBCx-92	EC docetaxel	IDC	BRCA2	74 (PD)	30 (PD)	90 (PD)	**93 (SD)**
HBCx-90	Paclitaxel	MBC	TP53	81 (PD)	35 (PD)	89 (PD)	0 (PD)
HBCx-95	FEC docetaxel	IDC	None	0 (PD)	32 (PD)	50 (PD)	**100 (R)**
HBCx-106	FEC docetaxel	IDC	TP53	75 (PD)	43 (PD)	69 (PD)	**90 (SD)**

IDC: invasive ductal carcinoma, MBC: metaplastic breast cancer, TGI: tumor growth inhibition, AC: Adriamycin + cyclophosphamide; FEC: 5-FU, epirubicin, cyclophosphamide; PD: progressive disease; SD: stable disease; R: regression; CR: complete response

Figure legends

Figure 1. Comparison between residual disease–derived PDX (RD) and primary tumors-derived PDX (PT). **A,** Percent tumor take in nude mice for residual tumors (*n*=53) and primary tumors (*n*= 919), by breast cancer subtype. * $p<0.01$, *** $p< 0.0001$, **** $p<0.00001$ (Fisher's exact test). **B,** Latency of TNBC PDX defined as the number of days between transplantation of the tumor and first outgrowth. ** $p< 0.001$ (unpaired *t*-test). **C,** MFS (metastasis-free survival) of patients compared to PDX latencies in the residual disease group. Metastasis-free survival (MFS) was defined as the time from surgery to the diagnosis of metastasis. **D,** Kaplan-Meier disease-free survival curves for patients in residual disease (RD) and primary tumors (PT) groups. **E,** Drug response of residual TNBC PDX as compared to primary tumors derived PDX: fraction of PDX models with a TGI ≥ 90% or < 90% after two cycles of chemotherapy (AC, docetaxel, cisplatin and capecitabine, one cycle lasts three weeks). *n*=10 PDX and *n*= 22 PDX in residual disease and primary tumors groups, respectively. **F,** Drug response curves of 3 residual TNBC PDX (HBCx-12A, HBCx-95 and HBCx-39) treated by AC, docetaxel, cisplatin and capecitabine (two three-week cycles). Mean of relative tumor volume (8-10 xenografts per group) ± SD. **G**, Individual tumor growth curves in control and capecitabine-treated xenografts.

Figure 2. Patient #63 history and PDX response to chemotherapy. **A,** Treatment of the patient and preclinical experiments on the HBCx-63 PDX. **P**atient #63 (59 years old) received four cycles of FEC100, followed by four cycles of docetaxel 100. At surgery, the HBCx-63 PDX was established from residual tumor tissue (Chevallier classification: grade 4). Lung metastasis were diagnosed 11 months after surgery: the patient was treated with three cycles of paclitaxel plus bevacizumab (first line). There was no response to treatment and the patient was switched onto second-line treatment with capecitabine (4 cycles). Metastatic disease progressed on capecitabine, with the occurrence of brain metastasis. The patient received carboplatin (third line) and then palliative care. The HBCx-63 PDX received the same sequence of treatment: 5-FU + navelbine, paclitaxel + bevacizumab, and

capecitabine. **B,** Waterfall plots representing the percent change in tumor volume for HBCx-63 PDX treated with 5-FU+ navelbine (adjuvant treatment), paclitaxel plus bevacizumab (first line) and capecitabine (second line). Two additional groups were added: capecitabine treatment of xenografts without prior treatment (adjuvant) and capecitabine treatment in xenografts previously treated with 5-FU + navelbine (first line). **C,** Immunohistochemistry analysis of TYMS (2.5X and 10X) in one representative xenograft of the control group, one xenograft treated by 5FU + navelbine and one xenograft treated by 5Fu+navelbine followed by paclitaxel + bevacizumab. The IHC analysis was performed on 3 different xenografts per group.

Figure 3. Biomarker analysis of the capecitabine response in 32 TNBC PDX. **A,** Waterfall plot representing the capecitabine response in 32 TNBC PDXs (10 derived from residual tumors and 22 from primary tumors). Each bar represents the median change in tumor volume from baseline in treated xenografts (*n*=8-10) after two three-week cycles of capecitabine treatment. Regression includes both partial responses and complete responses. **B,** Dendrogram (Ward linkage, Pearson distance) and heatmap based on genes differentially expressed between capecitabine-sensitive and capecitabine-resistant PDX. **C,** IHC analysis of RB expression in two resistant (HBCx-24 and HBCx-1) and two responding (HBCx-12A and HBCx-106) PDX (20X). **D,** Waterfall plot representing the capecitabine response in 32 TNBC PDXs according to RB status **E,** IHC analysis of TYMP expression in three resistant (HBCx-1, HBCx-90 and HBCx-66) and three responding (HBCx-92, HBCx-63 and HBCx-12A) PDX (20X). **F,** Association between TYMP H-score and the response to capecitabine in 32 TNBC PDX and combination of TYMP and RB biomarkers (Fisher's exact test).

Figure 4. Analysis of the correlation between tumor growth inhibition and changes in the expression of Rb-dependent proliferation-associated genes. **A,** tumor growth inhibition curves for seven TNBC PDX **B**, Percent TGI and heat-map representing fold-changes in normalized expression gene expression between control and treated xenografts (*n*=4) for eight Rb-dependent proliferation-

associated genes: *AURKA, PLK1, TTK, TOP2A, CCNB1, CCNA1, TK1* and *TYMS*. **C,** Plot of the correlation between fold-changes in gene expression and TGI. The Spearman correlation *p*-values obtained were as follows: 0.0056 (TK1), 0.0056 (TYMS), 0.0032 (CCNA2), 0.017 (CCNB1), 0.0032 (TOP2A), 0.0032 (TTK), 0.0349 (PLK1) and 0.0246 (AURKA).

Figure 5. siRNA-mediated inhibition of RB1 in a cell line established from the HBCx-12A PDX. **A,** In vivo response to capecitabine treatment of the residual HBCx-12A PDX. **B,** Cell viability assay of the HBCc-12A cell line treated by different concentration of 5-FU. The results are represented as the mean ± SD from experiments replicated three times. **C**, Western blot analysis of HBCc-12A cells treated with siControl and two different siRNA against RB1 and 5-FU (40 μM). **D,** cell viability assay of HBCc-12A cells treated by 5-FU and transfected with siControl, siRB1 and siRB2 siRNA. Results of 5-FU treated cells are normalized on siControl, siRB1 and siRB2 untreated cells and represented as fold change from siControl. Experiments were replicated three times.

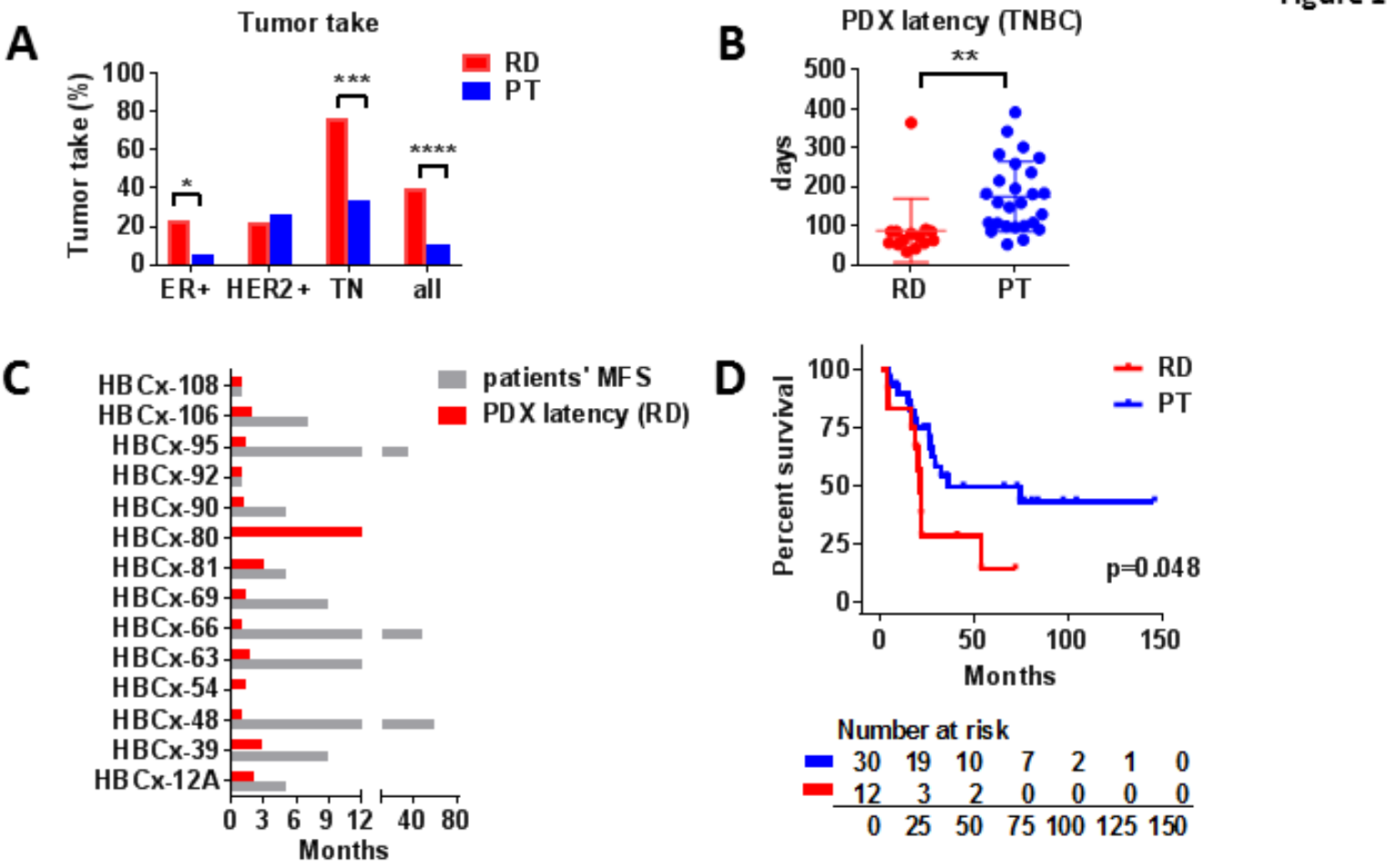

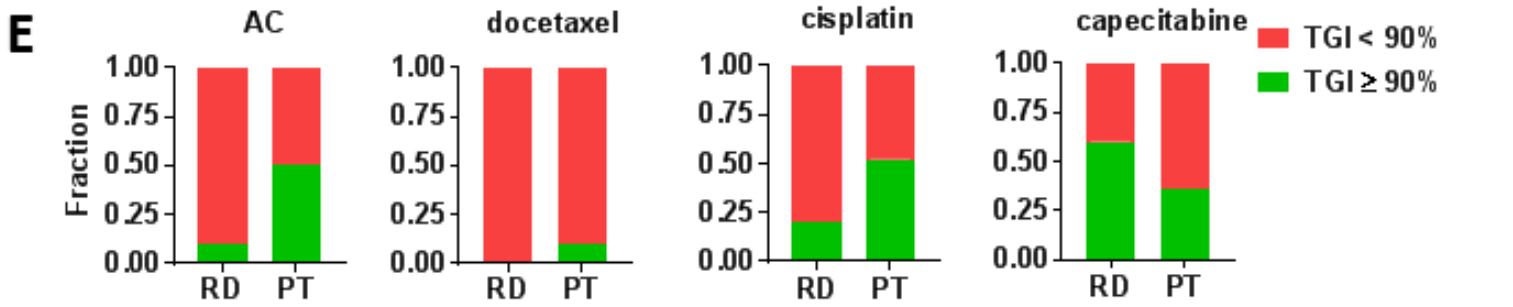

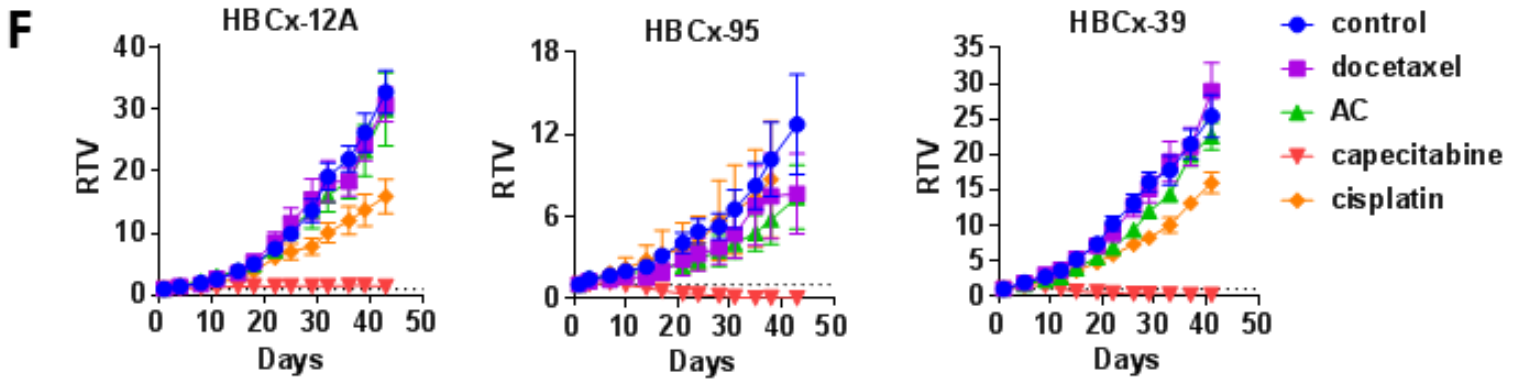

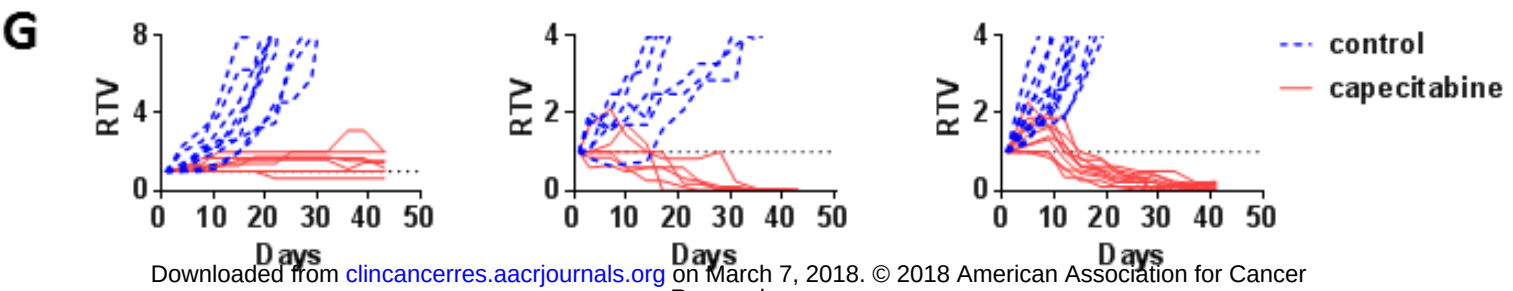

Figure 2

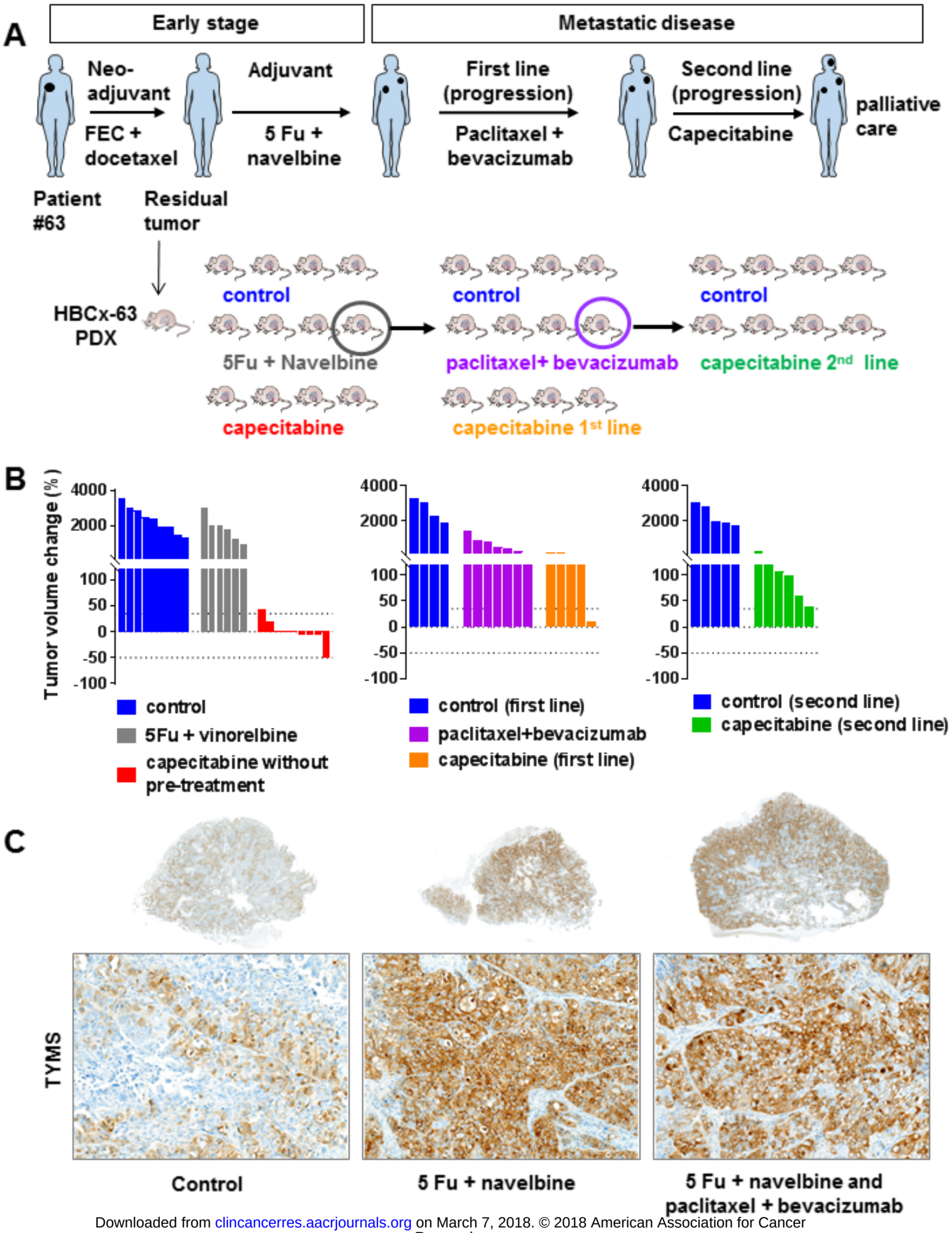

Figure 3

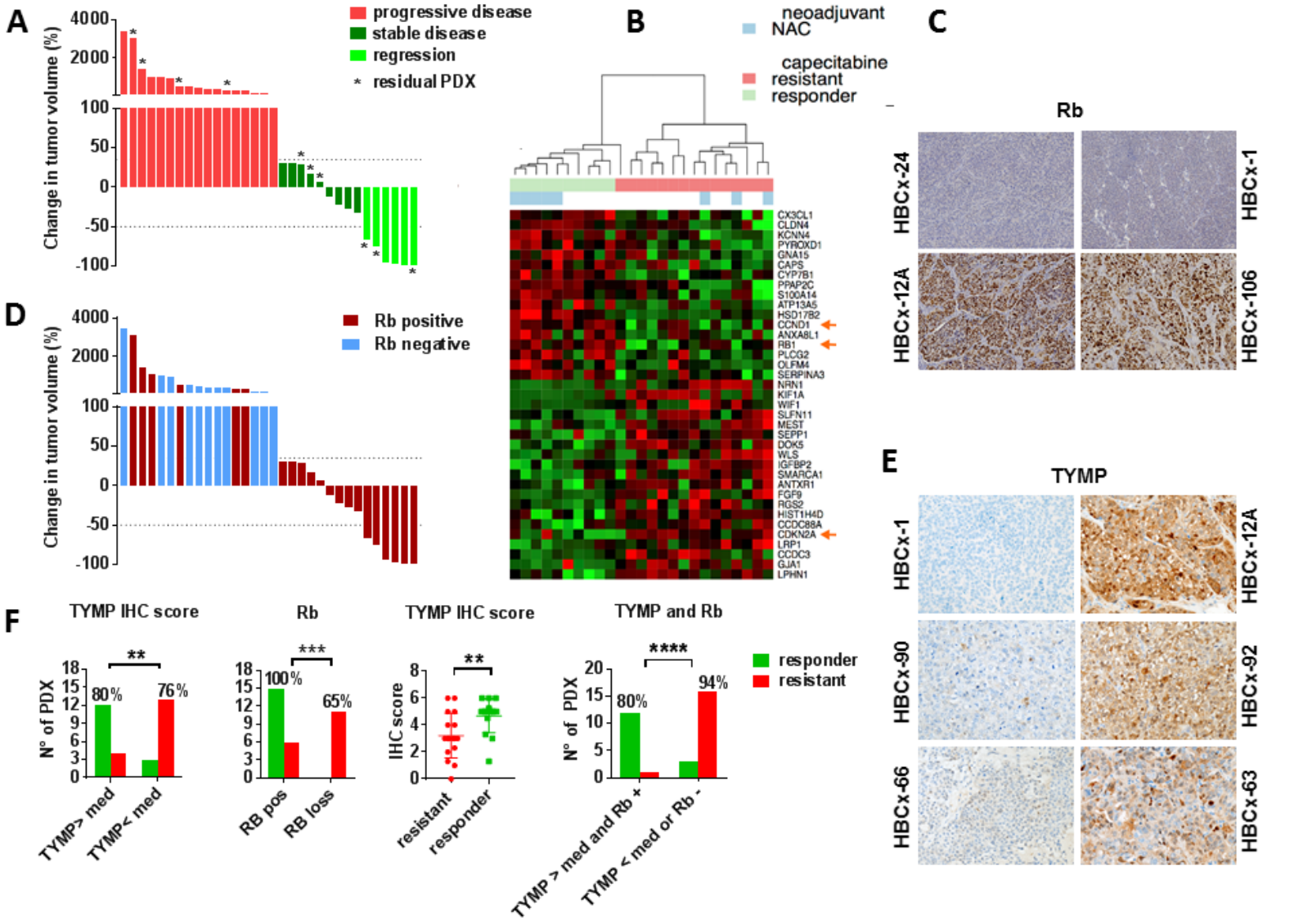

Figure 4

A

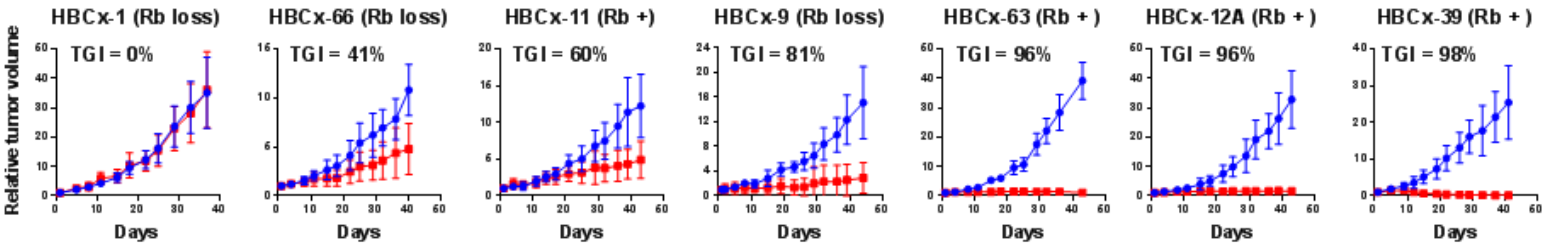

B

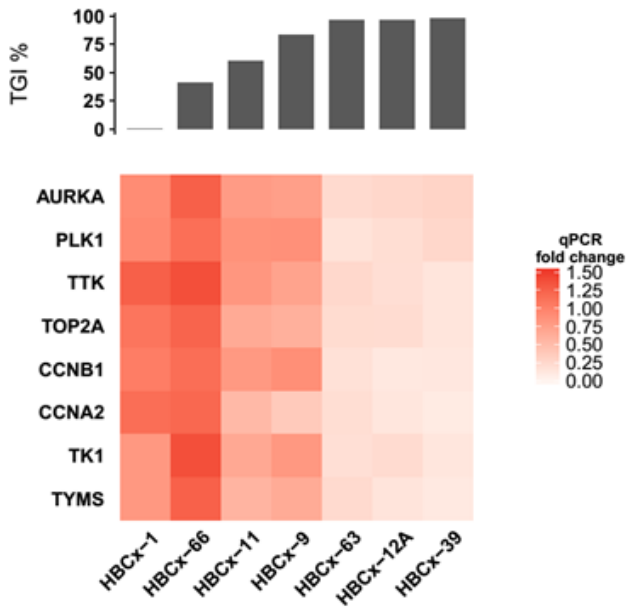

C

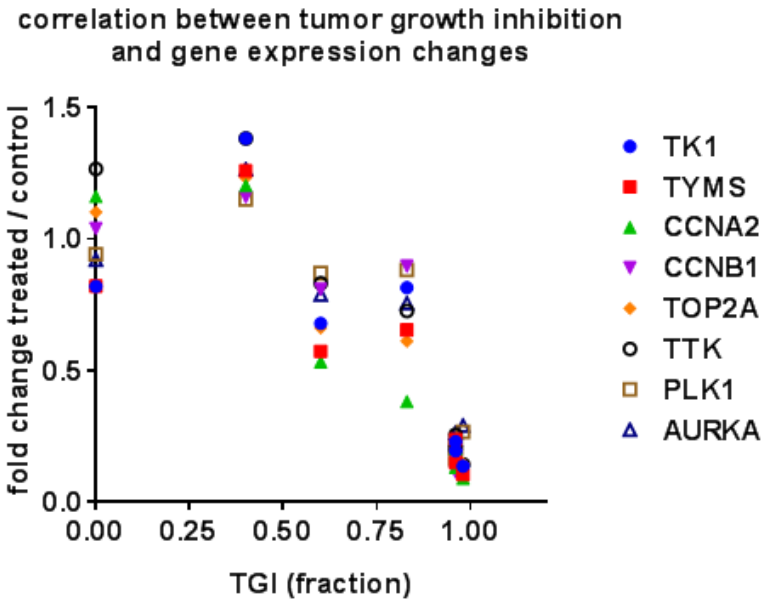

Figure 5

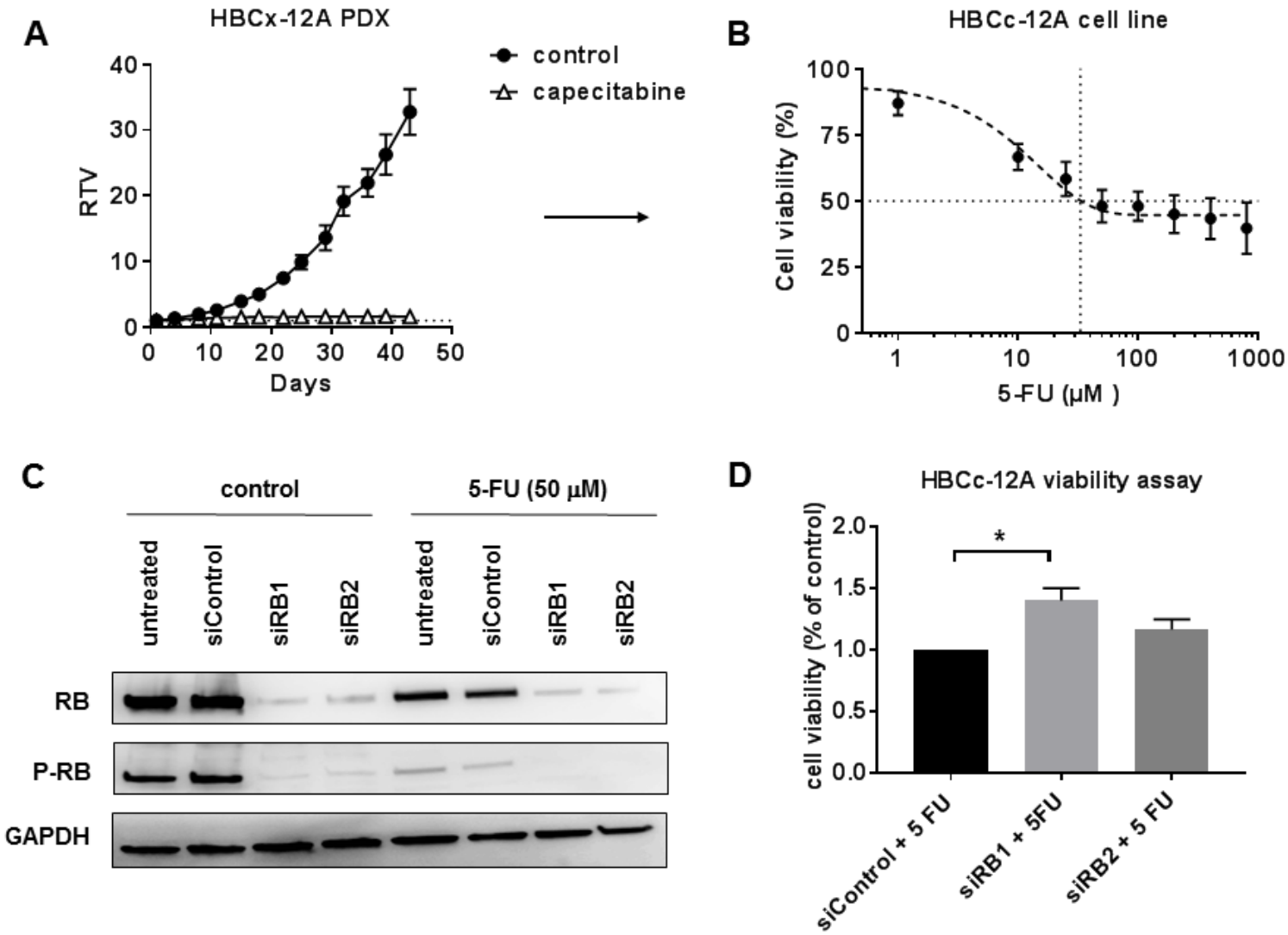

AACR American Association for Cancer Research

Clinical Cancer Research

Capecitabine efficacy is correlated with TYMP and RB expression in PDX established from triple-negative breast cancers

Elisabetta Marangoni, Cécile Laurent, Florence Coussy, et al.

Clin Cancer Res Published OnlineFirst February 20, 2018.